Polymer Chemistry

ELECTRONIC SUPPORTING INFORMATION

Quantifying bacterial adhesion on antifouling polymer brushes via Single-Cell Force Spectroscopy

Cesar Rodriguez-Emmenegger,[a,*] Sébastien Janel,[b] Andres de los Santos Pereira,[a] Michael Bruns,[c] and Frank Lafont[b] ,

Materials and methods

Materials

10-Undecen-1-ol (98%), trietyhlamine (99%), α-bromoisobutyryl bromide (98%), platinum(0)-1,3-divinyl-1,1,3,3-tetramethyldisiloxane (Karstedt's catalyst, 5% solution in xylene), trichlorosilane (99%), methacryloyl chloride (97%), oligo(ethylene glycol) methyl ether methacrylate (M_n = 300 g mol^{-1}, MeOEGMA), oligo(ethylene glycol) methacrylate (M_n = 500 g mol^{-1}, HOEGMA), 2-[(methacryloyloxy)ethyl]dimethyl-3-sulfopropyl ammonium hydroxide (SBMA, 97%), 2-methacryloyloxyethyl phosphorylcholine (PCMA, 97%), $CuBr_2$ (99%), $CuCl_2$ (99.999%), CuBr, (99.99%), CuCl (99.995%), 2,2'-bipyridyl (99%), 1,4,8,11-tetramethyl-1,4,8,11- tetraazacyclotetradecane (Me$_4$Cyclam, 98%), dopamine hydrochloride, human serum albumin (HSA, 99% by electrophoresis), and fibrinogen from human blood plasma (Fbg, 90%) were purchased from Sigma–Aldrich, Czech Republic. 3-[N-(Dimethylamino)propyl]acrylamide (98%) and DL-1-aminopropan-2-ol (98%) were acquired from TCI. β-Propiolactone was acquired from SERVA Electrophoresis. ω-Mercaptoundecyl bromoisobutyrate was synthesised by a previously published method.[1] Triethylamine was purified by distillation over calcium hydride before use.

Synthesis of silane-ATRP initiator

10-Undecen-1-yl-2-bromo-2-methylpropionate. The ATRP-initiator-functionalised alkene was prepared by a modified method from literature.[2] To a solution of 10-Undecen-1-ol (15 mL, 75 mmol) and triethylamine (13.5 mL, 90 mmol) in dry THF (75 mL) was added dropwise a solution of α-bromoisobutyryl bromide (10.7 mL) in 30 mL of dry THF at 0 ºC. The reaction mixture was kept under stirring overnight at room temperature. Hexane (150 mL) was subsequently added to the mixture and it was washed twice with 2 N HCl, twice with brine, and water, and dried over sodium sulphate. After removal of the solvent under vacuum, the product was purified by vacuum distillation. ^{1}H NMR (Bruker 300 MHz, CDCl$_3$) δ (ppm): 1.21-1.43 (m, 12H), 1.61-1.73 (m, 2H), 1.93 (s 6H), 2.03 (q, 2H, J = 7.2 Hz), 4.16 (t, 2H, J = 6.6 Hz). 4.87-5.04 (m, 2H). 5.72-5.9 (m, 1H).

(11-(2-Bromo-2-methyl)propionyloxy)undecyltrichlorosilane. To an Ar-filled dry flask containing 10-undecen-1-yl-2-bromo-2-methylpropionate (8.15 g, 25 mmol) and trichlorosilane (25.3 mL, 250 mmol) was added Karstedt's catalyst (500 ppm equivalent) and kept under stirring to react overnight. The mixture was quickly passed through a plug of silica to remove the catalyst and the remaining trichlorosilane was removed under reduced pressure. The product was purified by Kugelrohr distillation. ^{1}H NMR (300 MHz, CDCl$_3$) δ (ppm): 1.21-1.47 (m, 16H), 1.51-1.74 (m, 4H), 1.93 (s 6H), 4.16 (t, 2H, J = 7 Hz).
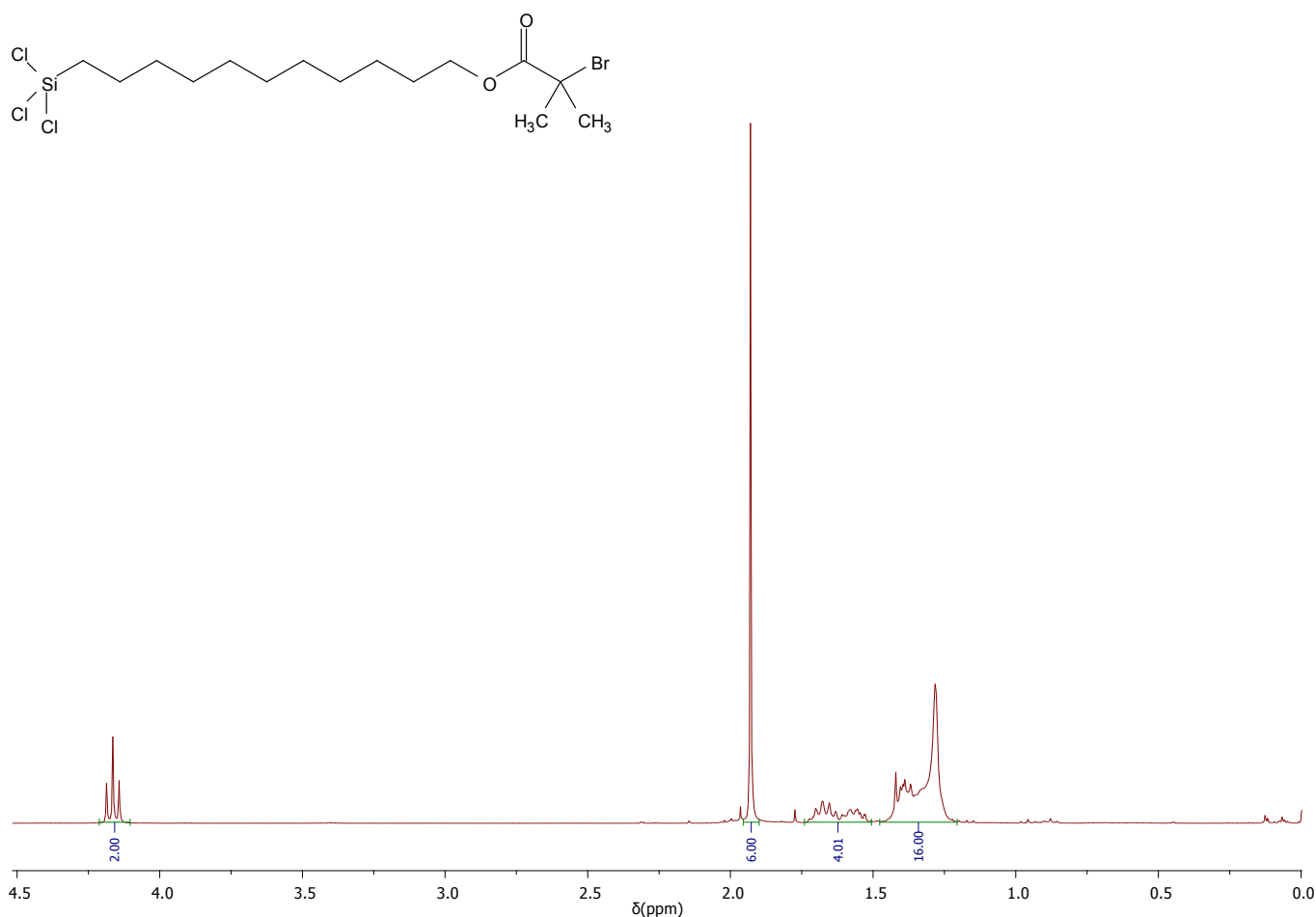
Fig. S1 ^{1}H NMR spectrum of (11-(2-Bromo-2-methyl)propionyloxy)undecyltrichlorosilane.

Synthesis of monomers

The monomers CBAA and HPMA employed for the growth of the corresponding polymer brushes were synthesised according to methods previously reported.[3]

(3-Acryloylaminopropyl)-(2-carboxyethyl)dimethylammonium (carboxybetaine acrylamide, CBAA). A solution of 3-[*N*-(dimethylamino)propyl]acrylamide (7.8 g, 55 mmol) in 100 mL of anhydrous THF was cooled to -20 ºC and subsequently a solution of β-propiolactone (5.0 g, 69 mmol) 40 mL of anhydrous THF dropwise under Ar atmosphere. The reaction was allowed

to proceed for 24 h at 4 ºC. The white precipitate was washed with dry THF and diethyl ether and dried under vacuum (yield: 80%). ^{1}H NMR (250 MHz, D$_2$O) δ (ppm): 6.32 (t, 1H), 6.2 (t, 1H), 5.87 (t, 1H), 3.66 (t, 2H), 3.48 (m, 4H), 3.17 (s, 6H), 2.75 (t, 2H)

N-(2-Hydroxypropyl)methacrylamide (HPMA). A mixture of 1-aminopropan-2-ol (66.3 g, 0.88 mol) and anhydrous sodium carbonate (106 g, 1 mol) in 250 mL of freshly distilled dichloromethane was cooled to 0 ºC. A solution of methacryloyl chloride (89.1 g, 0.85 mol) in 120 mL of dichloromethane added dropwise over 1 h under vigorous stirring. The reaction was allowed to proceed for a further 30 min. Subsequently 30 g of anhydrous sodium sulphate were added and the solids were filtered off. The filtrate was concentrated to half of the volume and the product was crystallised at -20 ºC and then recrystallised from acetone (yield: 80%).
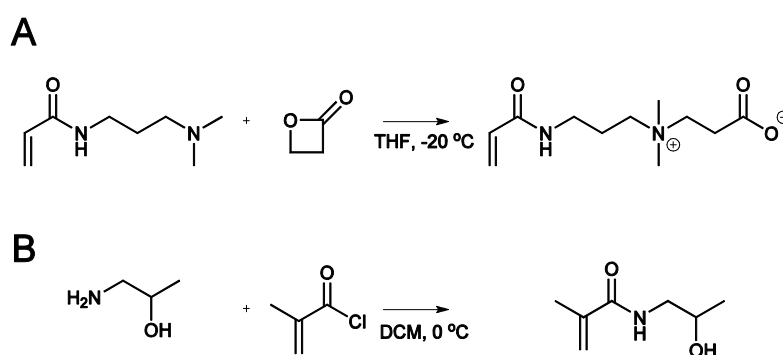
Scheme S1 Monomer synthesis. Synthesis of carboxybetaine acryl amide (A) and *N*-(2-hydroxypropyl)methacrylamide (B).

Methods

Ellipsometry. The dry layer thickness of the obtained polymer brushes was measured on silicon wafer chips due to the reflective nature of the Si-surface. The silicon chips were prepared in parallel with the glass substrates for SCFS measurement. The native SiO$_2$ layer on top of the Si-surface was found to have a thickness of 2.0 nm after cleaning. Ellipsometric measurements were performed using a Variable Angle Spectroscopic Imaging Auto-Nulling Ellipsometer EP^3-SE (Nanofilm Technologies GmbH, Germany) with a laser at a wavelength λ = 532 nm at angles of incidence AOI = 60, 65, and 70º in air at room temperature. The data were fitted using multilayer models with the EP4Model analysis software.

Contact angle. The dynamic water contact angles were measured by the sessile drop method with an OCA 20 contact angle goniometer (DataPhysics, Germany). A 5 µL water drop was deposited on the surface and the drop profile was recorded while the drop volume was increased by 10 µL and subsequently decreased by the same amount at a rate of 0.1 µL s^{-1}. The profiles were fitted with the tangent leaning method and the contact angles.

X-ray photoelectron spectroscopy (XPS). XPS measurements were carried out with a K-Alpha spectrometer (ThermoFisher Scientific). The samples were analysed using a micro-focussed, monochromated Al Kα X-ray source (400 µm spot size). The kinetic energy of the electrons was measured using a 180º hemispherical energy analyser operated in the constant analyser energy mode (CAE) at 50 eV pass energy for elemental spectra. Data acquisition and processing using the Thermo Advantage software is

described elsewhere.[4] The spectra were fitted with one or more Voigt profiles (binding energy uncertainty: ±0.2 eV). The analyser transmission function, Scofield sensitivity factors,[5] and effective attenuation lengths (EALs) for photoelectrons were applied for quantification. EALs were calculated using the standard TPP-2M formalism.[6] All spectra were referenced to the C1s peak of hydrocarbons at 285.0 eV binding energy controlled by means of the well-known photoelectron peaks of metallic Cu, Ag, and Au.

Surface plasmon resonance (SPR). The irreversible non-specific protein adsorption was measured with a spectroscopic SPR instrument based on the Kretschmann geometry (Institute of Photonics and Electronics, Czech Republic) at a temperature of 25 °C (±0.01 °C). The sensor response was recorded as the shift in the resonance wavelength of the surface plasmons. In a typical experiment, phosphate-buffered saline solution (PBS) was flown through the flow cell of the instrument by a peristaltic pump until the baseline was stable. Subsequently, the solution under study was injected for 15 min, followed by PBS for 60 min. The fouling response is the difference between the baselines before and after contact with the protein solutions and stabilisation in PBS. The adsorbed mass was obtained by calibration of the sensor response (a wavelength shift of 1 nm corresponds to a mass of adsorbed protein of 15 ng cm^{-2}).[7]

Preparation of the colloidal probe cantilever. A 10 μL drop of a dispersion of borosilicate microspheres (diameter 10 μm, 30 mg mL^{-1} in milliQ water) was deposited on a gold coated (50 nm thick) glass slide and allowed to dry. A tipless cantilever (TL-CONT, nanosensors, nominal spring constant 0.2 N m^{-1}) was cleaned using O$_2$ plasma (Diener Electronic Fempto 50% power, 15 min). The cantilever was mounted on an XYZ micro-translation stage and brought into contact with a single microsphere using a Bruker BioScope Catalyst mounted on a Zeiss AxioVert 200m microscope. The microsphere can be picked up thanks to the formation of a larger meniscus between the cantilver and the microsphere compared to the one between the gold surface and the microsphere. The cantilever was rapidly placed in a preheated oven and kept for 2 h at 780-820°C to fuse the microsphere.
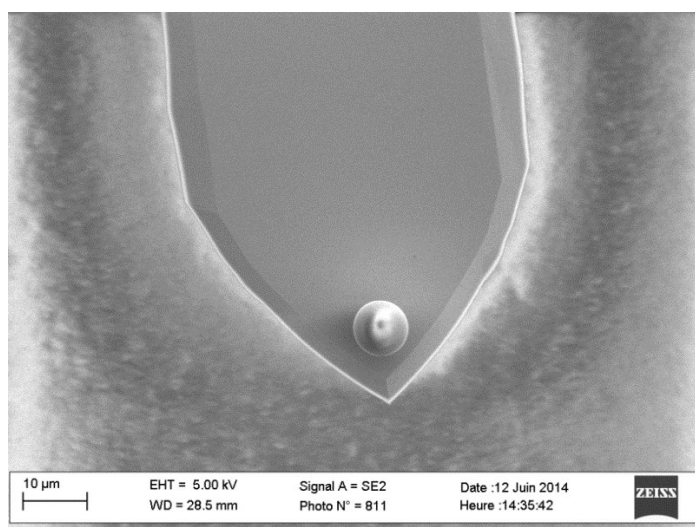
Fig. S2 SEM micrograph of the colloidal probe cantilever, proving the attachment of a single glass bead onto the cantilever.

Additional results of the characterisation of the layers

XPS of the initiator layer

The high resolution XPS spectrum of the C1s region of the silane-initiator adlayer on the surface shows a predominance of the peak at 285.0 eV corresponding to C-C and C-H of the alkane backbone of the initiator molecule. Furthermore, the C-O and O-C=O at 286.7 eV and 289.2 eV respectively correspond well to the ester expected for the initiator moiety.[7-9]

The Br3d spectrum confirms the presence of the initiator moiety. The detection of the Br $3d_{5/2}$ peak located at 67.7 eV may be associated with the formation of bromide ions via decomposition during the XPS analysis.[10-12] The contribution of the Na2s component arises from the glass substrate, which can still be observed as the adlayer is only 1.2 nm thick (penetration depth of the technique ≈10 nm).
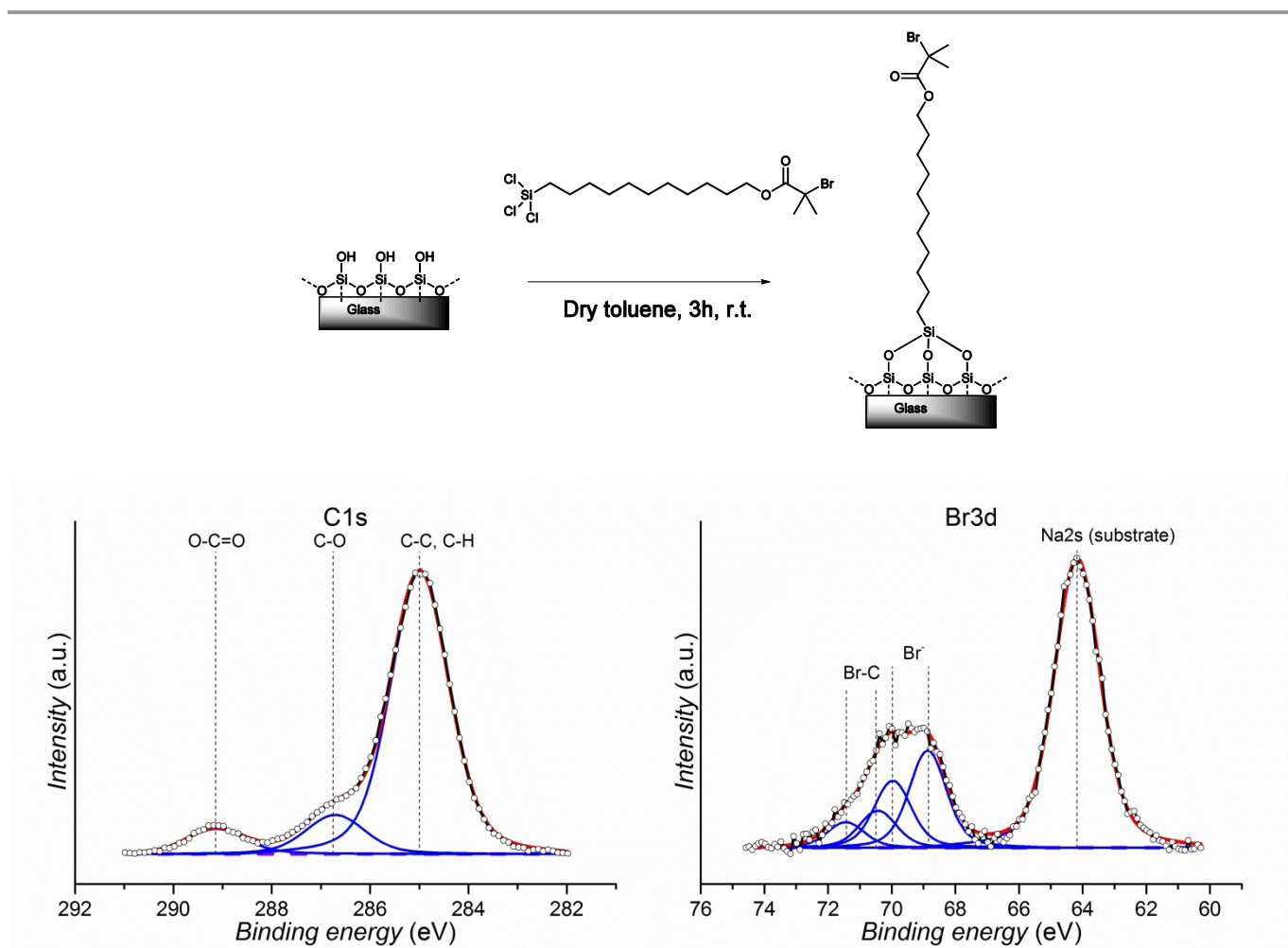
Fig S3 Immobilisation of initiator ad-layer. Reaction scheme (top) and high resolution XPS spectra of the obtained surface (bottom)

XPS spectra of the polymer brushes

The C1s spectra of the polymer brushes confirm the change in the chemical structure with respect to the silane-initiator ad-layer upon polymerisation.[7-9] The spectra of all methacrylate polymer brushes, poly(MeOEGMA), poly(HOEGMA), poly(HEMA), poly(PCMA), and poly(SBMA), show an ester peak at 289.0 eV (O-C=O). On the other hand poly(CBAA), an acrylamide, and poly(HPMA), a methacrylamide, present an amide peak around 287.9 eV. The spectra of poly(HOEGMA) and poly(MeOEGMA) show a predominance of the C-O peak at 286.4 eV arising from the oligo(ethylene glycol) side chains. In the case of poly(HEMA), this contribution is observed but is comparatively smaller, as it arises from a single ethylene glycol side group signal. A peak observed at 285.9 eV for poly(MeOEGMA), poly(HOEGMA), and poly(HEMA) corresponds to the tertiary carbon of the methacrylate backbone.

In the C1s spectrum of poly(HPMA) the component at 285.9 eV is larger, as it represents the overlap of the signals due to C-N and the tertiary carbon in the polymer backbone, while the C-O is still visible at 286.7 eV. In the case of poly(PCMA), both the C-N contribution of the quaternary ammonium group overlapped with the tertiary methacrylate carbon at 286.1 eV and the C-O from the ester side chain and phosphate at 286.8 eV are detected. In the case of poly(SBMA), the components for C-O, C-N, C-S, and tertiary carbon contribute to the same peak and cannot be distinguished.

No nitrogen was observed on the N1s spectra of the poly(MeOEGMA), poly(HOEGMA), poly(HEMA). On the other hand in the polymers presenting nitrogen two peaks appear. These arise either from the (meth)acrylamide (around 399.8 eV for poly(HPMA) and for poly(CBAA)) or from the positively charged quaternary ammonium group (around 402.5 eV for poly(PCMA), poly(CBAA), and poly(SBMA))[7, 13].

The S2p region of poly(SBMA) displays a peak at 167.3 eV confirming the presence of sulphur in the negatively charged C-$(SO_3)^-$ species.[14] Phosphorus is detected in poly(PCMA) by a peak at 133.0 eV in the P2p spectrum.[13] In both cases, the expected spin-orbit splitting ($2p_{1/2}$-$2p_{3/2}$) is observed.

Table S1 reports the measured relative atomic compositions and the predicted values calculated from the chemical formula of each polymer brush In all cases a good agreement was found, except for a slight excess of carbon, which can be attributed to adventitious contamination from laboratory air before measurement.

(A) Poly(MeOEGMA)   (B) Poly(HOEGMA)   (C) Poly(HEMA)   (D) Poly(HPMA)   (E) Poly(PCMA)   (F) Poly(CBAA)   (G) Poly(SBMA)
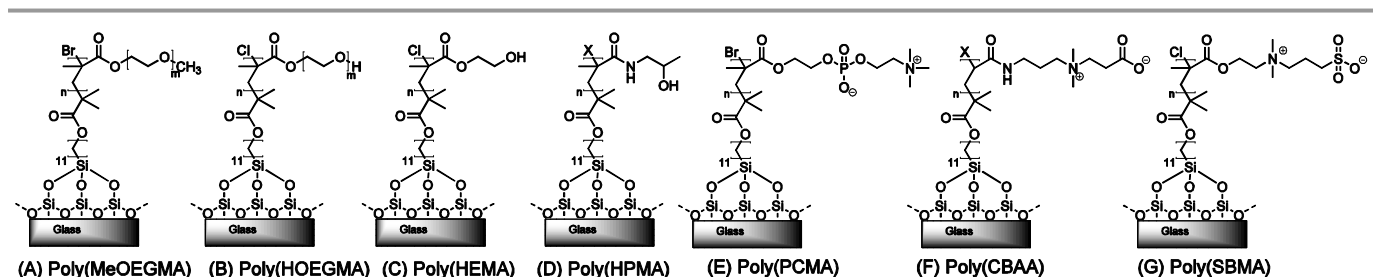
Scheme S2. Chemical structures of the polymer brushes
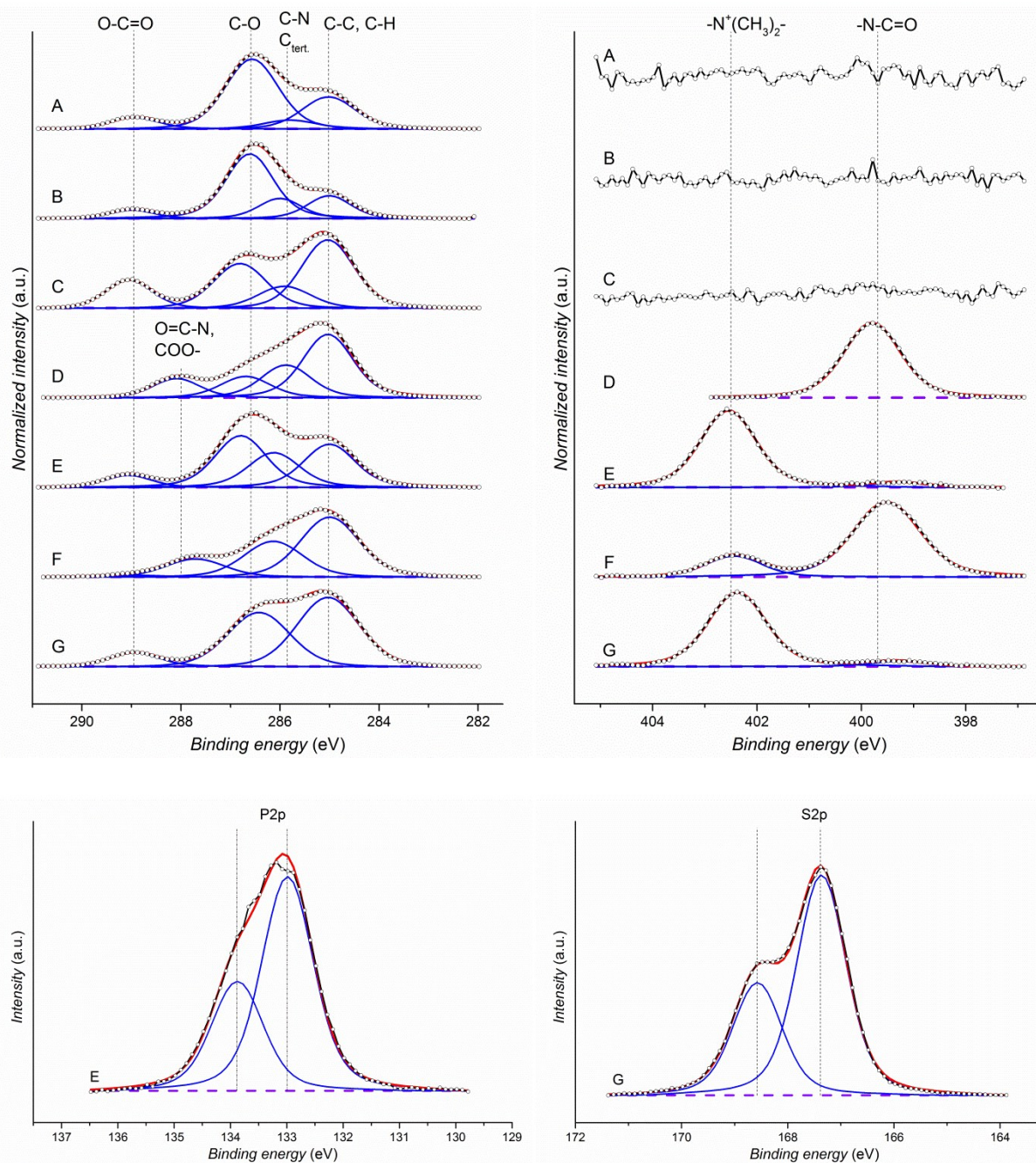
Fig. S4 Top: high resolution XPS of the C1s (left) and N1s (right) regions of the spectra of the polymer brushes: (A) poly(MeOEGMA), (B) poly(HOEGMA), (C) poly(HEMA), (D) poly(HPMA), (E) poly(PCMA), (F) poly(CBAA), and (G) poly(SBMA). Bottom: high resolution XPS of the P2p region of poly(PCMA) (left) and the S2p region of poly(SBMA).

Table S1. Comparison of the measured and the predicted relative atomic compositions of the polymer brushes by XPS.

Polymer	Relative % C		Relative % O		Relative % N		Relative % S		Relative % P	
	measured	predicted	measured	predicted	measured	predicted	measured	predicted	measured	predicted
Poly(MeOEGMA	70.4	68.3	29.6	31.7	0.0	0.0	0.0	0.0	0.0	0.0
Poly(HOEGMA)	68.4	66.7	31.6	33.3	0.0	0.0	0.0	0.0	0.0	0.0
Poly(HEMA)	68.7	66.7	31.3	33.3	0.0	0.0	0.0	0.0	0.0	0.0
Poly(HPMA)	71.1	70.0	19.2	20.0	9.7	10.0	0.0	0.0	0.0	0.0
Poly(PCMA)	63.9	57.9	25.6	31.6	4.8	5.3	0.0	0.0	5.7	5.3
Poly(CBAA)	71.3	68.8	16.5	18.8	12.2	12.5	0.0	0.0	0.0	0.0
Poly(SBMA)	64.4	61.1	24.4	27.8	5.2	5.6	6.0	5.6	0.0	0.0

AFM topography imaging of the surfaces
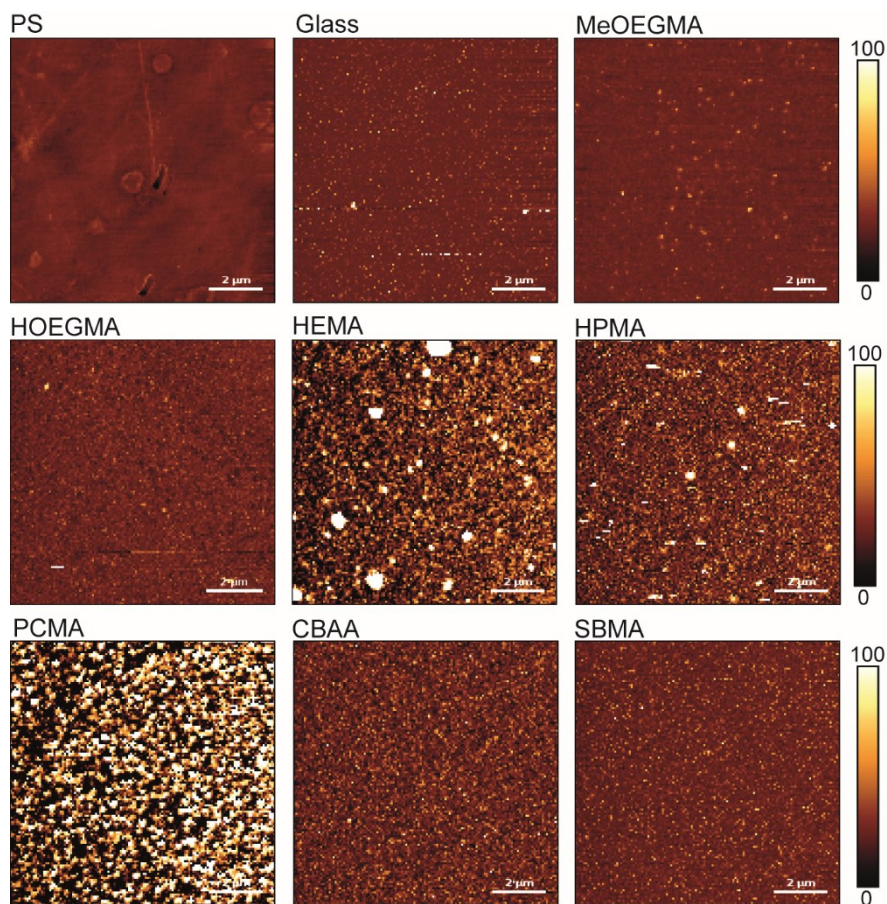
Fig. S5. AFM topography images of the surfaces. The images were acquired in QI mode in PBS (pH 7.4) at 37 ºC. The colour scale represents 100 Å.

AFM topography images were acquired in PBS at 37 °C, the same conditions employed for the single-bacterium adhesion experiments. The images show a homogenous coverage of the surfaces, with a roughness that is on a much smaller scale than the dry thickness of the layers. In aqueous solution the polymer brushes are known to swell and increase their thickness due to the uptake of solvent to a degree that depends on the chemical and physical structure of the brush.

Resistance to protein fouling

The resistance of the polymer brushes to non-specific protein adsorption was tested by surface plasmon resonance (SPR) according to established methods.[7] For this purpose, the polymer brushes were grown in parallel on gold-coated SPR chips from a self-assembled monolayer of ω-mercaptoundecyl bromoisobutyrate.[15] Solutions in PBS (pH 7.4) of human serum albumin (5 mg mL^{-1}) and fibrinogen (1 mg mL^{-1}) as well as undiluted blood plasma were flown over the surfaces in independent channels for 15 min, followed by PBS for 60 min. The fouling response is the difference between the baselines before and after contact with the protein solutions and is presented in Table S2, together with previously published results for the rest of the brushes and gold as a reference surface.

Table S2. Irreversible non-specific adsorption from single-protein solutions in PBS (pH 7.4) and full blood plasma measured by surface plasmon resonance after 15 min of contact and washing with PBS for 60 min.

Surface	Fouling (ng cm^{-2})		
	Human Serum Albumin (5 mg mL^{-1})	Fibrinogen (1 mg mL^{-1})	Human blood plasma (undiluted)
Gold (reference)[a]	126	321	306
Poly(MeOEGMA)[a]	0	0	18
Poly(HOEGMA)	0	0	22
Poly(HEMA)[a]	0	0	26
Poly(HPMA)[a]	0	0	0
Poly(PCMA)	0	0	308
Poly(CBAA)[a]	0	0	0
Poly(SBMA)	0	0	27

[a]: Previously reported.[7]

Confirmation of cell viability after SCFS

As a further proof that the bacterium was alive during the course of the measurements, the colloidal probe cantilever with the bacterium attached after the experiments was kept overnight at 28 ºC. The fluorescence image obtained subsequently showed that the bacterium had divided into multiple cells, confirming that it was still alive after the measurement of the force curves (Figure S5).
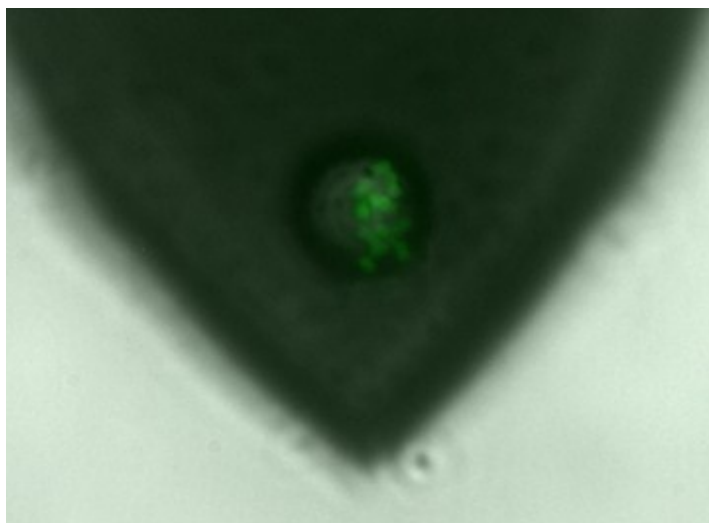
Fig. S6 Combined fluorescence and optical microscopy image of the colloidal probe cantilever with the bacterium immobilised after SCFS experiments and overnight incubation at 28 ºC. The single bacterium can be observed to have divided into multiple cells still on the colloidal probe proving that it was still alive.

Notes and references

^a Institute of Macromolecular Chemistry, Academy of Sciences of the Czech Republic, v.v.i., Heyrovsky sq. 2, 162 06 Prague, Czech Republic. E-mail: rodriguez@imc.cas.cz; Fax: +420 296 809 410; Tel: +420 296 809 333.

^b Cellular Microbiology and Physics of Infection Group, CNRS UMR 8204, INSERM U1019, Institut Pasteur de Lille, Lille University, Lille, France.

^c Institute for Applied Materials (IAM), Karlsruhe Nano Micro Facility (KNMF), Karlsruhe Institute of Technology (KIT), Hermann-von-Helmholtz-Platz 1, 76344 Eggenstein-Leopoldshafen, Germany

1. D. M. Jones, A. A. Brown and W. T. S. Huck, *Langmuir*, 2002, **18**, 1265-1269.
2. K. Matyjaszewski, P. J. Miller, N. Shukla, B. Immaraporn, A. Gelman, B. B. Luokala, T. M. Siclovan, G. Kickelbick, T. Vallant, H. Hoffmann and T. Pakula, *Macromolecules*, 1999, **32**, 8716-8724.
3. A. de los Santos Pereira, C. Rodriguez-Emmenegger, F. Surman, T. Riedel, A. B. Alles and E. Brynda, *RSC Advances*, 2014, **4**, 2318-2321.
4. B. Yameen, C. Rodriguez-Emmenegger, C. M. Preuss, O. Pop-Georgievski, E. Verveniotis, V. Trouillet, B. Rezek and C. Barner-Kowollik, *Chemical Communications*, 2013, **49**, 8623-8625.
5. J. H. Scofield, *J. Electron. Spectrosc. Relat. Phenom.*, 1976, **8**, 129-137.
6. S. Tanuma, C. J. Powell and D. R. Penn, *Surf Interface Anal*, 1994, **21**, 165-176.
7. F. Surman, T. Riedel, M. Bruns, N. Y. Kostina, Z. Sedláková and C. Rodriguez-Emmenegger, *Macromolecular Bioscience*, 2015, n/a-n/a.
8. C. Rodriguez-Emmenegger, C. M. Preuss, B. Yameen, O. Pop-Georgievski, M. Bachmann, J. O. Mueller, M. Bruns, A. S. Goldmann, M. Bastmeyer and C. Barner-Kowollik, *Advanced Materials*, 2013, **25**, 6123-6127.
9. E. H. Lock, D. Y. Petrovykh, P. Mack, T. Carney, R. G. White, S. G. Walton and R. F. Fernsler, *Langmuir*, 2010, **26**, 8857-8868.
10. S. A. Al-Bataineh, L. G. Britcher and H. J. Griesser, *Surf. Interface Anal.*, 2006, **38**, 1512-1518.
11. S. A. Al-Bataineh, L. G. Britcher and H. J. Griesser, *Surf. Sci.*, 2006, **600**, 952-962.

12. B. Yameen, N. Zydziak, S. M. Weidner, M. Bruns and C. Barner-Kowollik, *Macromolecules*, 2013, **46**, 2606-2615.
13. K. Sugiyama and K. Ohga, *Macromolecular Chemistry and Physics*, 1999, **200**, 1439-1445.
14. F. Zhang, E. T. Kang, K. G. Neoh, P. Wang and K. L. Tan, *Biomaterials*, 2001, **22**, 1541-1548.
15. T. Riedel, C. Rodriguez-Emmenegger, A. de los Santos Pereira, A. Bědajánková, P. Jinoch, P. M. Boltovets and E. Brynda, *Biosensors and Bioelectronics*, 2013, **55C**, 278-284.